HHS Public Access

Author manuscript

Ergonomics. Author manuscript; available in PMC 2024 October 29.

Published in final edited form as:

Ergonomics. 2024 February ; 67(2): 182–193. doi:10.1080/00140139.2023.2216408.

Flexible sensor-based biomechanical evaluation of low-back exoskeleton use in lifting

Wei Yin[a], **Yinong Chen**[b], **Curran Reddy**[c], **Liying Zheng**[d], **Ranjana K. Mehta**[a], **Xudong Zhang**[a,b,c]

[a]Department of Industrial and Systems Engineering, Texas A&M University, College Station, TX, USA

[b]Department of Mechanical Engineering, Texas A&M University, College Station, TX, USA

[c]Department of Biomedical Engineering, Texas A&M University, College Station, TX, USA

[d]Health Effects Laboratory Division, National Institute for Occupational Safety and Health, Morgantown, WV, USA

Abstract

This study aimed to establish an ambulatory field-friendly system based on miniaturised wireless flexible sensors for studying the biomechanics of human-exoskeleton interactions. Twelve healthy adults performed symmetric lifting with and without a passive low-back exoskeleton, while their movements were tracked using both a flexible sensor system and a conventional motion capture (MoCap) system synchronously. Novel algorithms were developed to convert the raw acceleration, gyroscope, and biopotential signals from the flexible sensors into kinematic and dynamic measures. Results showed that these measures were highly correlated with those obtained from the MoCap system and discerned the effects of the exoskeleton, including increased peak lumbar flexion, decreased peak hip flexion, and decreased lumbar flexion moment and back muscle activities. The study demonstrated the promise of an integrated flexible sensor-based system for biomechanics and ergonomics field studies as well as the efficacy of exoskeleton in relieving the low-back stress associated with manual lifting.

PRACTITIONER SUMMARY

This study established and tested a flexible sensor-based ambulatory system for biomechanical evaluation of human-exoskeleton interactions and as a promising new tool for field ergonomics studies in practical or naturalistic settings.

Keywords

Flexible sensors; human-exoskeleton interaction; low-back exoskeleton; lifting

CONTACT Xudong Zhang, xudongzhang@tamu.edu, Department of Industrial and Systems Engineering, Texas A&M University, 4077 Emerging Technologies Building, 3131 TAMU, College Station, TX 77843-3131, USA.

1. Introduction

Work-related musculoskeletal disorders (WMSD) account for about 25% of the total workers' compensation cost in the US (Liberty-Mutual 2017), approximately 40% (95,690 out of 247,620) of which are low-back injuries (BLS 2021). Exoskeletons, wearable devices intended to augment, enable, or enhance human physical capabilities, are populating workplaces as a potential means to prevent musculoskeletal injuries. Low-back exoskeletons are designed to reduce mechanical loading on the low-back while preserving the functionality and mobility of workers during tasks involving bending and lifting.

Exoskeletons can be categorised as active or passive (Wesslén 2018), and passive low-back exoskeletons have been increasingly adopted to assist manual materials handling tasks due to their relatively low cost and ease of use (MacDougall 2014). Muscle activity and kinematics measurements of the lumbar region are commonly acquired in demonstrating the efficacy or assessing the benefits of exoskeletons (Zheng et al. 2021). Previous studies have examined the effects of passive low-back exoskeletons using surface electromyography (EMG) and reported reduced back muscle activity as a result of wearing the exoskeletons (Abdoli-E, Agnew, and Stevenson 2006; Abdoli-e and Stevenson 2008; Alemi et al. 2019; Bosch et al. 2016; de Looze et al. 2016; Graham, Agnew, and Stevenson 2009; Hwang et al. 2021; Lotz et al. 2009; Madinei et al. 2020; Ulrey and Fathallah 2013; von Glinski et al. 2019). However, a reduction in back muscle activity alone does not necessarily imply a reduction in spine loading, especially when a significant lumbar kinematics change also accompanies the use of an exoskeleton. This is due to the flexion-relaxation effect (Koopman et al. 2019; Ulrey and Fathallah 2013) that occurs when in substantial trunk bending, passive tissues are stretched far enough to generate a major portion of the required extension moment such that back muscles are de-activated (Floyd and Silver 1955). Furthermore, it is often difficult to weigh the trade-offs between observed benefits and costs such as reduced muscle activation versus mechanical load transfer. Therefore, a comprehensive understanding of biomechanical risks and benefits associated with the use of exoskeletons necessitates a deeper, model-based analysis of the underlying mechanical loads and in particular the loads experienced by the lumbar spine.

Conventional joint kinematics and dynamics measurements and analyses often employ optical motion capture systems and force plates. However, optical motion capture systems require marker visibility and thus have limited applicability in assessing human-exoskeleton interactions since the exoskeletons may obstruct surface markers over areas of interest such as the trunk and pelvis. In some studies, reflective markers were placed on the exoskeleton to approximate the human motion (Weston et al. 2018), which may jeopardise the quality of the data and validity of the findings. Some other studies used cluster markers, attached to the pelvis using bandages and connecting rods to estimate participants' lumbar motion (Koopman et al. 2019, 2020). Such a strategy, nevertheless, may interfere with or alter subjects' performance and significantly bias the measurements. Inertial-magnetic sensors can provide a cost-effective alternative with no visibility restriction, but their applications have been hampered by issues such as performance interference and data artefact due to their size and the way they are attached to the body (Yin et al. 2021). For example, once an

inertial measurement unit (IMU) wearable sensor is attached to a body region or segment, it would inhibit the addition and proper use of a wearable assistive device such as exoskeleton.

A new technology of wireless, miniaturised, skin-mounted, multimode sensors, in particular BioStamp nPoint (MC10, Inc., MA, USA), has shown its great promise in addressing the above-stated challenges. Its flexible design allows for direct body-conforming adhesion to the skin surfaces. This sensor integrates an accelerometer, gyroscope, and biopotential measurement unit and can be controlled with a tablet through a Bluetooth connection without any additional hardware, thus supporting potential ambulatory data recording for both laboratory and field studies (Sen-Gupta et al. 2019). Several recent studies have demonstrated the viability of these flexible sensors for measuring simple gait parameters (e.g. stride numbers, stride time) (Moon et al. 2017) and body kinematics (Jeong et al. 2021; Yin et al. 2021), and assessing physical activity or stress in clinical and field studies (Sen-Gupta et al. 2019; Zahabi et al. 2022). Most recently, a preliminary study further explored the applicatin of flexible sensors in acquiring lifting kinematics and kinetics estimates and discerning the effects of a back exoskeleton (Yin et al. 2022).

Therefore, the objective of this study was twofold. The first objective was to develop a flexible sensor-based system for measuring the torso, low-back, and lower-extremity kinematics and low-back dynamics and muscle activity and establish its concurrent validity by comparing the measures with those from a simultaneously deployed conventional optical motion capture system. The second objective was to demonstrate the utility of the proposed flexible sensor-based system by a biomechanical evaluation of passive low-back exoskeleton use in lifting and pave the way for future field or on-site studies of the human- exoskeleton interactions.

2. Materials and methods

2.1. Subjects and experimental protocol

Twelve healthy individuals, six males and six females (age: 25± 4 years, weight: 65.9± 9.7kg, height: 1.72± 0.07m), all free from any musculoskeletal conditions or disorders at the time of the experiment, were recruited to serve as the subjects. The study was approved by the Institutional Review Board of Texas A&M University. After providing written informed consent, subjects were given sufficient time to become familiar with the exoskeleton and its use in the experiment.

Each flexible sensor unit integrates a six-axis accelerometer (±16g) and a gyroscope (±2000°/s) for motion data acquisition, and a biopotential component (±0.2V), which was used for EMG measurement (note: a single unit however cannot be used for recording all three signals concurrently). A total of eleven Biostamp nPoint sensors were placed on the subject (Figure 1): four for measuring the surface EMG with a sampling rate of 1000Hz at the following sites bilaterally: thoracic erector spinae (TES, 5cm bilateral to the T9 spinous process) and lumbar erector spinae (LES, 3cm bilateral to the L3 spinous process) (McGill 1991); and seven used to acquire kinematics data for multiple segments (Figure 1a,b). The seven sensors for kinematic measurement with a sampling rate of 125Hz were strategically placed: two were attached to T12 and sacrum (S1 spinous processes) to measure the lumbar

flexion/extension motion; four were attached to the lateral aspect of the thighs and shanks, as recommended by Yin et al. (2021), for capturing the knee and ankle flexion/extension motions; one was placed on the sternum, below the suprasternal notch, to allow for low-back exoskeleton flexion angle calculation in relation to the thigh sensors; sensors on the sacrum and thigh segments were intended to estimate the left and right hip flexion/extension. With sensors placed, subjects went through a calibration procedure consisting of a series of hip abduction/adduction movements without any motion of the other joints as described in Appendix A.

Spherical reflective markers were attached to anatomical landmarks based on the plug-in gait marker set, as depicted in Figure 1a,b. A twelve-camera Vicon system (Vicon Motion Systems Ltd, Oxford, UK) was used to record the motions of surface markers at a sampling rate of 50Hz. Of note is that the Vicon system was only in use when the subjects were not wearing the exoskeleton because the markers in the low back region (e.g. ones on the anterior superior iliac spine) would have been obstructed or interfered by the exoskeleton. In addition, the ground reaction forces data were recorded by two AMTI force plates (Advanced Mechanical Technology, Inc., MA, USA) at a sample rate of 1000Hz. Before experimental trials, a predefined right shank kickback motion was repeated three times to synchronise the time of Vicon system and BioStamp sensors.

The passive low-back exoskeleton utilised in the study was a Laevo V2.5 (Figure 2). Buckles on the suspenders were adjusted for subjects of different anthropometry such that no pressure on the shoulders was felt; the hip paddings were affixed to the pelvis by balancing and tightening the front, back, and buttock belts such that the leg pads were properly centred. The initial Laevo spring-loaded joint (Figure 2) flexion angle was set to 0° which indicated the device not providing any support when the user stood upright.

Subjects were instructed to perform a squat lifting task with a 6kg box from the ground to waist height while standing on two force plates (Figure 3). Based on the NIOSH lifting equation and the weight of the box, the task had a lifting index value of approximately 0.5, confirming a minimal risk associated with the task (Waters et al. 1993). The box, 32 × 31.5 × 31.5cm with hand cut-outs 26cm off the ground, was placed in front of the subject at a self-selected distance (Figure 3). Subjects were required to start in a stationary standing position, feet shoulder-width apart, and to hold the box for 5–10s after squat lifting to the waist height with self-selected speed. This lifting task was performed WITH and WITHOUT wearing the exoskeleton and repeated five times with 1-min breaks. The sequence of each condition was randomly assigned to each subject with six subjects (three males, three females) performing the lifting under condition WITH first, and the other six under condition WITHOUT first. Prior to the experimental trials, subjects were asked to perform a calibration lifting trial without the exoskeleton (the same as the experimental trials) that would be used to establish the baseline for normalisation of the EMG signals for each muscle under each condition.

2.2. Data processing and analysis

Gyroscopic and acceleration data captured by the sensors were used to estimate joint flexion/extension angles, namely the lumbar spine, hips, knees, and ankles, using algorithms

detailed in Appendix A. OpenSim, an open musculoskeletal modelling software system, was employed to build subject-specific models and then derive marker-based joint kinematics with a full-body lumbar spine (FBLS) model (Raabe and Chaudhari 2016). A dynamic linked model was then built based on the subject-specific OpenSim model and a bottom-up segment orientation-based estimation method adapted from Faber, Kingma, and van Dieën (2010) was used to calculate the L5S1 flexion/extension moments from both marker-based and flexible sensor-based kinematics by solving the following equations:

$$\sum \boldsymbol{F} + \sum m\boldsymbol{g} + \sum m\boldsymbol{a} = 0$$
$$\sum \boldsymbol{F} \times \boldsymbol{r} + \sum \boldsymbol{M} + \sum I\boldsymbol{\alpha} = 0$$

where $\boldsymbol{F}$ denotes all external forces applied at the body segment; m is the segment mass; $\boldsymbol{g}$ is the gravity; $\boldsymbol{a}$ represents the segment linear acceleration; $\boldsymbol{r}$ is the vector from the point of application of force to the joint centre; $\boldsymbol{M}$ denotes all external moments; I is the moment of inertial of each segment and $\boldsymbol{\alpha}$ is the segment angular acceleration. In both approaches to estimating L5S1 flexion/extension moments, kinematics of the body segments were used together with the ground reaction forces, and the L5S1 moment estimations were presented in pelvic coordinate system. For the trials under condition WITH, the external force generated by the exoskeleton was estimated using Laevo angle-torque relationship measured by Koopman et al. (2019) and the exoskeleton flexion angle calculated by sensors placed on the sternum and thighs.

The sensor- and marker-based joint kinematics and L5S1 flexion/extension moments were truncated to only include the lifting phase (Figure 3), from starting bending to starting holding the box statically, which was determined by the sensor on T12 using a threshold for detecting static frame. A moving window of 25 frames (0.2s) was adopted to scan the motion signals, and then the mean acceleration in the window was calculated and compared with the threshold to infer whether the sensor or segment was static. The threshold was decided through a small-scale independent pilot test, and we identified that a threshold of 0.08g for acceleration data can efficiently detect static frames for each sensor on each segment.

EMG data were first filtered using a fourth-order band-pass Butterworth filter (10–400Hz) (Zahabi et al. 2022). Then, the data were truncated to only include the lifting task and smoothed using the Root Mean Square (RMS) with a moving window of 125ms. Finally, the EMG data of LES and TES were averaged over sides and normalised by the peak EMG magnitude (95th percentile) of the data captured from the pre-experimental lifting trial (%baseline). The peak normalised EMG (90th percentile) values of each muscle were extracted and utilised to evaluate the effect of the low-back exoskeleton on back muscle activity (Hwang et al. 2021; Jonsson 1982).

2.3. Statistical analysis

Angles of hip, knee, and ankle were averaged across both sides. The root-mean-square error (RMSE) and Pearson's correlation coefficient (r) between sensor- and marker-based measurements for tasks without the exoskeleton were calculated for each subject

to investigate the validity of the proposed flexible sensor-based method. Sensor-based measurement was then employed to inspect the effects of the exoskeleton on lumbar, hip, knee, and ankle flexion/extension, and L5S1 flexion/extension moments, in which paired *t*-tests were utilised and the mean peak joint angles and moments of each subject across all five trials with or without the exoskeleton were the response variables. Paired *t*-tests were also employed to examine the effects on back muscle activity with the mean peak normalised EMG values of each subject across all five trials, with or without the exoskeleton, being the response variables. A significance level of 0.05 was used for *t*-tests.

3. Results

3.1. Validation of flexible sensor-based measurements

The grand mean RMSE (and *r*) between sensor- and marker-based measurements across all subjects was 7.67° (0.954), 4.80° (0.995), 3.99° (0.997), 3.39° (0.995), and 21.02N·m (0.926) for the lumbar, hip, knee, and ankle flexion, and L5S1 flexion moment, respectively, as summarised in Table 1. Representative joint kinematics and L5S1 moment profiles from one subject (subject #3) whose metrics were close to the overall means are shown in Figure 4.

3.2. Effects of the low-back exoskeleton

Wearing the exoskeleton during lifting led to significantly increased peak lumbar flexion (by 1.4–27.6°), reduced peak hip flexion (by 1.7–25.4°), and reduced peak L5S1 flexion moment (by 15.84–53.05 N·m), as suggested by the paired *t*-test results (Table 2). No significant differences were detected for knee and ankle flexion. The joint kinematics and L5S1 moments profiles of a representative subject (subject #3) with and without the exoskeleton are shown in Figure 5. Significantly reduced back muscle activities of both LES and TES—by 2.4–29.4% and 2.0–37.4%, respectively—in exoskeleton-assisted lifting were also identified (Table 3).

4. Discussion

This study established a flexible sensor-based system capable of measuring the lumbar, hip, knee, and ankle joint kinematics and L5S1 flexion moment during a symmetric lifting task, and investigated its validity by comparing to a simultaneously deployed conventional marker-based motion capture system. Results indicated that the proposed new system yielded excellent agreement with the marker-based system (r>0.90) (Poitras et al. 2019), whereas the RMSEs appeared to be more variable across joints.

With regard to the joint angle estimation, as defined by Cuesta-Vargas, Galán-Mercant, and Williams (2010) and Poitras et al. (2019), a RMSE of <5° is considered as excellent and between 5° and 10° as good. Based on that criterion, the proposed method achieved good to excellent agreement with the marker-based approach for the hip, knee, and ankle joints. However, the results for the lumbar spine showed poorer agreement than the other joints. The lumbar spine joint also had the lowest r-value compared with the other joints. Larger RMSE and lower correlation coefficient in estimating pelvic orientation when subjects performed tasks involving substantial pelvic movement (e.g. sit-to-stand transfers,

with RMSE = 8.9° and $r = 0.92$) have been previously reported (Bolink et al. 2016). This may have been attributable to the excessive soft tissue artefact associated with the markers attached to the pelvic region when the subjects were in a low, squatting position. Additionally, when the subjects attained the lowest squatting position, markers on the left and right ASIS might have been completely obstructed by the abdominal pannus and thigh and substantial gap-filling required in motion tracking could have introduced more error. In contrast, the skin-integrated flexible sensors attached to the sacrum and T12 spinal landmarks incur less soft tissue artefact and are immune to the visual blockage problem. The joint kinematics profiles of all subjects were consistent (with the ones in Figure 4) in showing a greater discrepancy in the lumbar flexion profiles compared with other joints, especially during 40–60% time of completion when the subject reached the lowest position. Of note is that the marker-based measurements here were not used as the 'gold standard' but rather a reference line. The accuracy of the proposed sensor-based method in kinematic measurement would have to be assessed by a comparison with real 'ground truth' acquired by *in vivo* dynamic X-ray imaging as has been done for marker-based methods (Li et al. 2012). The estimation of L5S1 flexion moment using the proposed sensor-based system also generated poorer agreement with the marker-based method than the estimated hip, knee, and ankle kinematics. This could be due to the accumulation of errors in calculating hip, knee, and ankle joint kinematics because, in the bottom-up estimation method, L5S1 flexion moment was calculated by iterating the motions of lower segments (Faber, Kingma, and van Dieën 2010).

The sensor calibration procedure could have been another potential source of error. The anatomical standing position was used to calibrate the sensors' coordinate systems in which the joint angles were presumed to be zero, as defined by the OpenSim model. The hip abduction/adduction movement was used to calibrate the sensor attached to lower extremities, in which the knee joint was assumed to be motionless and the hip joint was assumed to undergo abduction/adduction only. Neither however could be precisely controlled, and offsets would thus be created if the subject did not execute the predefined position or motion correctly. Additionally, the inaccuracy in attaching sensors to the sacrum and T12 could also have contributed to deviation of sensor calibration because the sensor's Z-axis was assumed to be in the sagittal plane of sacrum and T12.

The proposed method achieved overall a comparable level of accuracy in simulating hip, knee, and ankle joint kinematics (Al-Amri et al. 2018; Lebel et al. 2017; McGrath, Fineman, and Stirling 2018; Robert-Lachaine et al. 2017; Seel, Raisch, and Schauer 2014; Yin et al. 2021). Some studies obtained better agreement with marker-based measurement for pelvic orientation or lumbar spine angles (Bauer et al. 2015; Godwin, Agnew, and Stevenson 2009; Mjosund et al. 2017; Robert-Lachaine et al. 2017); however, the reported performances were limited to quasi-static motions or motions that did not involve substantial pelvic movement. Bolink et al. (2016) reported larger RMSE and smaller r in estimating pelvic orientation for sit-to-stand transfers than for gait, which might be attributed to the inaccuracy of marker-based simulation as discussed above. The performance of the proposed method for L5S1 flexion moment estimation was comparable or better than those reported in previous studies using a video-based system (Mehrizi et al. 2019), the orientation-based method (Faber, Kingma, and van Dieën 2010), and inertial-magnetic sensors (Faber et al. 2020; Koopman

et al. 2018). Although the current study relied on force plates to capture the ground reaction forces and moments, the proposed system could be integrated with instrumented shoes or pressure insoles to enable ambulatory measurement of L5S1 joint moments. Most relevant studies that adopted inertial-magnetic sensors had limited applications in naturalistic settings due to the sensors' size and the way they are attached to the body (Al-Amri et al. 2018; Bauer et al. 2015; Faber et al. 2020; Godwin, Agnew, and Stevenson 2009; Koopman et al. 2018; Lebel et al. 2017; McGrath, Fineman, and Stirling 2018; Mjosund et al. 2017; Robert-Lachaine et al. 2017; Seel, Raisch, and Schauer 2014). By contrast, flexible sensor-based studies have so far not identified any issues on sensor wearability, subject comfort, or performance interference (Moon et al. 2017; Sen-Gupta et al. 2019), encouraging further, more assertive exploration of this technology in field evaluation of human-exoskeleton or human-wearable interactions.

The effects of a passive low-back exoskeleton on users' lower body joint kinematics, L5S1 flexion moments, and back muscles were investigated using our proposed flexible sensor-based system. The observed increased peak lumbar flexion and decreased peak L5S1 flexion moments due to exoskeleton use were consistent with the prior research (Bosch et al. 2016; Hwang et al. 2021; Koopman et al. 2020; Koopman et al. 2019) on the same device. However, our results showed larger variability in the increase of lumbar flexion (by 1.4–27.6°) and the reduction of L5S1 flexion moments (by 15.84–53.05 N·m) which could be explained by the fact that the present study did not control the relative lifting positions such that each subject might perform a different percentage of the lumbar flexion range of motion. Some studies, however, reported reduced or constant lumbar flexion when subjects wore exoskeletons (Picchiotti et al. 2019; Ulrey and Fathallah 2013), which might be due to subtle differences in devices or task constraints.

To our knowledge, this was the first study that reported the changes in lumbar, hip, knee, and ankle flexion, and L5S1 flexion moment simultaneously. Apart from significantly increased lumbar flexion and reduced L5S1 flexion moment, our study identified significantly decreased hip flexion and decreased knee flexion (p=0.067, marginally significant). Aberrations in thigh segments were also found by von Glinski et al. (2019), in which significantly increased quadriceps femoris activity when users wore a low-back exoskeleton was reported. Similar mechanical load shifts or transfers were also identified in the evaluation of other passive exoskeletons (e.g. Weston et al. (2018)). Thus, the impacts of low-back exoskeletons on biomechanics of the lower extremities may warrant more investigative attention in future studies.

Significant reductions of back muscle EMG amplitude (mean reduction: 15.9% for LES, 12.8% for TES) were detected. The amount of reduction indicated smaller effects of the exoskeleton on reducing back muscle activity during lifting in comparison with other studies or other devices that showed mean reductions of more than 30% (Abdoli-E, Agnew, and Stevenson 2006; Abdoli-e and Stevenson 2008; Alemi et al. 2019). However, it should be noted that, due to the flexion-relaxation phenomenon, EMG reduction did not necessarily indicate back muscle load reduction (Koopman et al. 2019; Ulrey and Fathallah 2013). Since Abdoli-E, Agnew, and Stevenson (2006) and Alemi et al. (2019) did not report either lumbar flexion or L5S1 loads, it is unclear whether the exoskeletons being investigated

were effective in reducing low-back load, which underscores the importance of assessing the L5S1 joint loading when evaluating the efficacy of low-back exoskeletons.

Several limitations of this study are acknowledged. First, because the BioStamp nPoint sensors are not yet capable of acquiring the global orientation information, the proposed system presently can only measure joint motions in a single plane (e.g. the sagittal plan in this study). A new set of algorithms and calibration procedures would be needed to derive 3D joint kinematics estimates based on the flexible sensors. Secondly, the proposed system configuration, including the number of sensors and their placement strategy, was designed for estimating lumbar and lower limb dynamics for the evaluation of low-back exoskeletons. The configuration would need to be modified and optimised for investigations focussed more on the upper body and upper extremities. Lastly, while our aim was to develop a completely laboratory-free system, the current approach still required the involvement of force plates, which are laboratory-bound. Future endeavours will integrate the proposed system with instrumented shoes or pressure insoles to enable completely ambulatory biomechanical measurement for evaluating human-exoskeleton interactions in the field.

5. Conclusion

In conclusion, this study explored a flexible sensor-based ambulatory system for acquiring biomechanical data during human-exoskeleton interactions. Results demonstrated that the proposed system was able to generate biodynamic measures comparable to marker-based measurements and discern the effects of a passive low-back exoskeleton on body kinematics, L5S1 moment, and back muscle activity.

Funding

The author(s) reported there is no funding associated with the work featured in this article.

Disclosure statement

The findings and conclusions in this report are those of the authors and do not necessarily represent the official position of the National Institute for Occupational Safety and Health (NIOSH), Centres for Disease Control and Prevention (CDC). Mention of any company or product does not constitute endorsement by NIOSH/CDC.

Appendix A. Joint kinematics estimation algorithm

When wearable sensors were used to estimate human kinematics, converting motion data recorded in sensors' local coordinate systems into anatomically meaningful and interpretable information was an inevitable step. This study utilised several calibration procedures to calculate the transformation matrix for data conversion.

In order to be consistent with the segments' coordinate systems (B) defined in the OpenSim model (Raabe and Chaudhari 2016), the anatomical standing position (as shown in Figure 1a) was used to implement coordinate system alignment, through which, the Y-axis of each segment's coordinate system in the corresponding sensor's local coordinate system (S) could be obtained using the acceleration signals, as shown in Equation (1), where i represented the number of sensors, with 1, 2, 3, 4, 5, 6 denoting the sensor attached to T12, sacrum, left thigh, left shank, right thigh, and right shank, respectively, $\mathbf{Y}_i^S$ denoted the Y-axis of segment

i expressed in S of sensor *i*, $\mathbf{a}_i^S$ denoted the acceleration signal of sensor *i* expressed in S, and ‖ denoted the Euclidean norm.

$$\mathbf{Y}_i^S = -\mathbf{a}_i^S / \|\mathbf{a}_i^S\|, i = 1, 2, 3, 4, 5, 6. \tag{1}$$

For sensors on T12 and sacrum, assuming their Z axes (Figure 1c) were in the sagittal plane, their X and Z axes of each segment's coordinate system in the corresponding sensor's local coordinate system could be estimated as,

$$\begin{cases} \mathbf{Z}_i^S = \mathrm{Y}_i^S \times \mathbf{c} \\ \mathbf{X}_i^S = \mathrm{Y}_i^S \times \mathbf{Z}_i^S, i = 1, 2, \\ \mathbf{c} = [0, 0, 1] \end{cases} \tag{2}$$

where $\mathbf{X}_i^S$ and $\mathbf{Z}_i^S$ denoted the X and Z axes of segment *i* expressed in S of sensor *i*, **c** denoted the unit vector of Z-axis of sensor *i*.

Figure A1.
The hip abduction/adduction movement for calibrating flexible sensors on the lower limbs.

For sensors on the lower limbs, a hip abduction/adduction movement without any movement of the other joints (Figure A1) was utilised to estimate the abduction/adduction axis of rotation, $\mathbf{j}_i^S$, i=3,4,5,6, of each thigh and shank, which was assumed to be in the segment's sagittal plane. The $\mathbf{j}_i^S$ could be acquired using sensors' gyroscopic data and principal component analysis as demonstrated by McGrath, Fineman, and Stirling (2018)

and Yin et al. (2021). Then, their X and Z axes of each segment's coordinate system in the corresponding sensor's local coordinate system could be obtained using the following equation,

$$\begin{cases} \mathbf{Z}_i^S = \mathbf{j}_i^S \times \mathbf{Y}_i^S \\ \mathbf{X}_i^S = \mathbf{Y}_i^S \times \mathbf{Z}_i^S \end{cases}, i = 3, 4, 5, 6. \tag{3}$$

The transformation matrix $\mathbf{T}_{S,i}^B$, expressed in the sensor coordinate system with respect to the segment's coordinate system, could then be estimated as follows,

$$\mathbf{T}_{S,i}^B = \left[\mathbf{X}_i^S; \mathbf{Y}_i^S; \mathbf{Z}_i^S\right], i = 1, 2, 3, 4, 5, 6. \tag{4}$$

Next, the motion data recorded in sensors' local coordinate systems were converted into segments' anatomical coordinate systems by the following equation,

$$\begin{cases} \mathbf{a}_i^B = \mathbf{T}_{S,i}^B \cdot \mathbf{a}_i^S \\ \mathbf{g}_i^B = \mathbf{T}_{S,i}^B \cdot \mathbf{g}_i^S \end{cases}, i = 1, 2, 3, 4, 5, 6, \tag{5}$$

where $\mathbf{g}_i^B$ and $\mathbf{g}_i^S$ denoted the gyroscopic data from sensor i expressed in B and S, respectively, $\mathbf{a}_i^B$ and $\mathbf{a}_i^S$ denoted the acceleration data from sensor i expressed in B and S, respectively.

After the segment's body acceleration and gyroscopic information were obtained by Equation (5), the joint flexion/extension angular velocity could be derived by the subtraction between the gyroscopic data in the Z direction of the segments articulated by the joint. The joint flexion/extension angle could then be estimated by integrating its angular velocity, which, however, might result in drift due to sensors' random error (Yin et al. 2021). Thus, additional approaches were needed to remove the drift. Since the targeted task of this study was lifting, some static frames, with zero acceleration (gravity removed) and angular rate, before and after the task could always be located, during which the inclination angle of each segment with respect to the direction of gravity could be obtained by calculating the arctangent of the acceleration direction as shown in Equation (6), where θ_i denoted the inclination angle of segment i, x_i^B and y_i^B were the X and Y components of gravity in the body coordinate system of segment i.

$$\theta_i = \arctan\left(x_i^B / y_i^B\right), i = 1, 2, 3, 4, 5, 6. \tag{6}$$

Then, the joint flexion/extension angles during the static frames could be obtained and would be used to estimate the offset through a least-squares method. Finally, the estimated

offset angles were added to the integrated results, yielding joint angle estimation with less drift.

Abbreviations:

MoCap	motion capture
WMSD	Work-related musculoskeletal disorders
EMG	electromyography
IMU	inertial measurement unit
TES	thoracic erector spinae
LES	lumbar erector spinae
WITH	tasks performed with wearing the exoskeleton
WITHOUT	tasks performed without wearing the exoskeleton
RMS	root mean square
RMSE	root-mean-square error
r	Pearson's correlation coefficient
ASIS	anterior superior iliac spine

References

Abdoli-E M, Agnew MJ, and Stevenson JM. 2006. "An on-Body Personal Lift Augmentation Device (PLAD) Reduces EMG Amplitude of Erector Spinae during Lifting Tasks." Clinical Biomechanics 21 (5): 456–465. doi:10.1016/j.clinbiomech.2005.12.021. [PubMed: 16494978]

Abdoli-e M, and Stevenson JM. 2008. "The Effect of on-Body Lift Assistive Device on the Lumbar 3D Dynamic Moments and EMG during Asymmetric Freestyle Lifting." Clinical Biomechanics 23 (3): 372–380. doi:10.1016/j.clinbiomech.2007.10.012. [PubMed: 18093709]

Al-Amri M, Nicholas K, Button K, Sparkes V, Sheeran L, and Davies JL. 2018. "Inertial Measurement Units for Clinical Movement Analysis: Reliability and Concurrent Validity." Sensors 18 (3): 719. doi:10.3390/s18030719. [PubMed: 29495600]

Alemi MM, Geissinger J, Simon AA, Chang SE, and Asbeck AT. 2019. "A Passive Exoskeleton Reduces Peak and Mean EMG during Symmetric and Asymmetric Lifting." Journal of Electromyography and Kinesiology 47: 25–34. doi:10.1016/j.jelekin.2019.05.003. [PubMed: 31108346]

Bauer CM, Rast FM, Ernst MJ, Kool J, Oetiker S, Rissanen SM, Suni JH, and Kankaanpää M. 2015. "Concurrent Validity and Reliability of a Novel Wireless Inertial Measurement System to Assess Trunk Movement." Journal of Electromyography and Kinesiology 25 (5): 782–790. doi:10.1016/j.jelekin.2015.06.001. [PubMed: 26126796]

BLS. 2021. "Employer-Reported Workplace Injuries and Illnesses–2020." https://www.bls.gov/news.release/pdf/osh.pdf

Bolink SA, Naisas H, Senden R, Essers H, Heyligers IC, Meijer K, and Grimm B. 2016. "Validity of an Inertial Measurement Unit to Assess Pelvic Orientation Angles during Gait, Sit-Stand Transfers and Step-up Transfers: Comparison with an Optoelectronic Motion Capture System." Medical Engineering & Physics 38 (3): 225–231. doi:10.1016/j.medengphy.2015.11.009. [PubMed: 26711470]

Bosch T, van Eck J, Knitel K, and de Looze M. 2016. “The Effects of a Passive Exoskeleton on Muscle Activity, Discomfort and Endurance Time in Forward Bending Work.” Applied Ergonomics 54: 212–217. doi:10.1016/j.apergo.2015.12.003. [PubMed: 26851481]

Cuesta-Vargas AI, Galán-Mercant A, and Williams JM. 2010. “The Use of Inertial Sensors System for Human Motion Analysis.” Physical Therapy Reviews 15 (6): 462–473. doi:10.1179/1743288X11Y.0000000006. [PubMed: 23565045]

de Looze Michiel P., Bosch Tim, Krause Frank, Stadler Konrad S., and O’Sullivan Leonard W.. 2016. “Exoskeletons for Industrial Application and Their Potential Effects on Physical Work Load.” Ergonomics 59 (5): 671–681. doi:10.1080/00140139.2015.1081988. [PubMed: 26444053]

Faber GS, Kingma I, Chang CC, Dennerlein JT, and van Dieën JH. 2020. “Validation of a Wearable System for 3D Ambulatory L5/S1 Moment Assessment during Manual Lifting Using Instrumented Shoes and an Inertial Sensor Suit.” Journal of Biomechanics 102: 109671. doi:10.1016/j.jbiomech.2020.109671. [PubMed: 32143885]

Faber Gert S., Kingma Idsart, and van Dieën Jaap H.. 2010. “Bottom-up Estimation of Joint Moments during Manual Lifting Using Orientation Sensors instead of Position Sensors.” Journal of Biomechanics 43 (7): 1432–1436. doi:10.1016/j.jbiomech.2010.01.019. [PubMed: 20189574]

Floyd WF, and Silver PHS. 1955. “The Function of the Erectores Spinae Muscles in Certain Movements and Postures in Man.” The Journal of Physiology 129 (1): 184–203. doi:10.1113/jphysiol.1955.sp005347. [PubMed: 13252593]

Godwin A, Agnew M, and Stevenson J. 2009. “Accuracy of Inertial Motion Sensors in Static, Quasistatic, and Complex Dynamic Motion.” Journal of Biomechanical Engineering 131 (11): 114501. doi:10.1115/1.4000109. [PubMed: 20353265]

Graham RB, Agnew MJ, and Stevenson JM. 2009. “Effectiveness of an on-Body Lifting Aid at Reducing Low Back Physical Demands during an Automotive Assembly Task: assessment of EMG Response and User Acceptability.” Applied Ergonomics 40 (5): 936–942. doi:10.1016/j.apergo.2009.01.006. [PubMed: 19223026]

Hwang J, Kumar Yerriboina VN, Ari H, and Kim JH. 2021. “Effects of Passive Back-Support Exoskeletons on Physical Demands and Usability during Patient Transfer Tasks.” Applied Ergonomics 93: 103373. doi:10.1016/j.apergo.2021.103373. [PubMed: 33516046]

Jeong Hyoyoung, Kwak Sung Soo, Sohn Seokwoo, Lee Jong Yoon, Lee Young Joong, O’Brien Megan K., Park Yoonseok, Avila Raudel, Kim Jin-Tae, Yoo Jae-Young, Irie Masahiro, Jang Hokyung, Ouyang Wei, Shawen Nicholas, Kang Youn J., Kim Seung Sik, Tzavelis Andreas, Lee KunHyuck, Andersen Rachel A., Huang Yonggang, Jayaraman Arun, Davis Matthew M., Shanley Thomas, Wakschlag Lauren S., Krogh-Jespersen Sheila, Xu Shuai, Ryan Shirley W., Lieber Richard L., and Rogers John A.. 2021. “Miniaturized Wireless, Skin-Integrated Sensor Networks for Quantifying Full-Body Movement Behaviors and Vital Signs in Infants.” Proceedings of the National Academy of Sciences 118 (43): e2104925118. doi:10.1073/pnas.2104925118.

Jonsson B 1982. “Measurement and Evaluation of Local Muscular Strain in the Shoulder during Constrained Work.” Journal of Human Ergology 11 (1): 73–88. [PubMed: 7186516]

Koopman Axel S., Kingma Idsart, de Looze Michiel P., and van Dieën Jaap H.. 2020. “Effects of a Passive Back Exoskeleton on the Mechanical Loading of the Low-Back during Symmetric Lifting.” Journal of Biomechanics 102: 109486. doi:10.1016/j.jbiomech.2019.109486. [PubMed: 31718821]

Koopman Axel S., Kingma Idsart, Faber Gert S., Bornmann Jonas, and van Dieën Jaap H.. 2018. “Estimating the L5S1 Flexion/Extension Moment in Symmetrical Lifting Using a Simplified Ambulatory Measurement System.” Journal of Biomechanics 70: 242–248. doi:10.1016/j.jbiomech.2017.10.001. [PubMed: 29054609]

Koopman Axel S., Kingma Idsart, Faber Gert S., de Looze Michiel P., and van Dieën Jaap H.. 2019. “Effects of a Passive Exoskeleton on the Mechanical Loading of the Low Back in Static Holding Tasks.” Journal of Biomechanics 83: 97–103. doi:10.1016/j.jbiomech.2018.11.033. [PubMed: 30514627]

Lebel K, Boissy P, Nguyen H, and Duval C. 2017. “Inertial Measurement Systems for Segments and Joints Kinematics Assessment: Towards an Understanding of the Variations in Sensors Accuracy.” BioMedical Engineering OnLine 16 (1) doi:10.1186/s12938-017-0347-6.

Li K, Zheng L, Tashman S, and Zhang X. 2012. “The Inaccuracy of Surface-Measured Model-Derived Tibiofemoral Kinematics.” Journal of Biomechanics 45 (15): 2719–2723. doi:10.1016/j.jbiomech.2012.08.007. [PubMed: 22964018]

Liberty-Mutual. 2017. “Liberty Mutual Workplace Safety Index 2017.” https://business.libertymutualgroup.com/business-insurance/Documents/Services/Workplace%20Safety%20Index.pdf

Lotz CA, Agnew MJ, Godwin AA, and Stevenson JM. 2009. “The Effect of an on-Body Personal Lift Assist Device (PLAD) on Fatigue during a Repetitive Lifting Task.” Journal of Electromyography and Kinesiology 19 (2): 331–340. doi:10.1016/j.jelekin.2007.08.006. [PubMed: 18055220]

MacDougall W 2014. “Industrie 4.0: Smart Manufacturing for the Future.” Germany Trade & Invest. https://www.pac.gr/bcm/uploads/industrie4-0-smart-manufacturing-for-the-future-en.pdf

Madinei S, Alemi MM, Kim S, Srinivasan D, and Nussbaum MA. 2020. “Biomechanical Assessment of Two Back-Support Exoskeletons in Symmetric and Asymmetric Repetitive Lifting with Moderate Postural Demands.” Applied Ergonomics 88: 103156. doi:10.1016/j.apergo.2020.103156. [PubMed: 32678776]

McGill SM 1991. “Electromyographic Activity of the Abdominal and Low Back Musculature during the Generation of Isometric and Dynamic Axial Trunk Torque: Implications for Lumbar Mechanics.” Journal of Orthopaedic Research 9 (1): 91–103. doi:10.1002/jor.1100090112. [PubMed: 1824571]

McGrath T, Fineman R, and Stirling L. 2018. “An Auto-Calibrating Knee Flexion-Extension Axis Estimator Using Principal Component Analysis with Inertial Sensors.” Sensors 18 (6): 1882. doi:10.3390/s18061882. [PubMed: 29890667]

Mehrizi R, Peng X, Metaxas DN, Xu X, Zhang S, and Li K. 2019. “Predicting 3-D Lower Back Joint Load in Lifting: A Deep Pose Estimation Approach.” IEEE Transactions on Human-Machine Systems 49 (1): 85–94. doi:10.1109/THMS.2018.2884811.

Mjosund HL, Boyle E, Kjaer P, Mieritz RM, Skallgard T, and Kent P. 2017. “Clinically Acceptable Agreement between the ViMove Wireless Motion Sensor System and the Vicon Motion Capture System When Measuring Lumbar Region Inclination Motion in the Sagittal and Coronal Planes.” BMC Musculoskeletal Disorders 18 (1): 124. doi:10.1186/s12891-017-1489-1. [PubMed: 28327115]

Moon Yaejin, McGinnis Ryan S., Seagers Kirsten, Motl Robert W., Sheth Nirav, Wright John A., Ghaffari Roozbeh, and Sosnoff Jacob J.. 2017. “Monitoring Gait in Multiple Sclerosis with Novel Wearable Motion Sensors.” PLoS One 12 (2): e0171346. doi:10.1371/journal.pone.0171346. [PubMed: 28178288]

Picchiotti MT, Weston EB, Knapik GG, Dufour JS, and Marras WS. 2019. “Impact of Two Postural Assist Exoskeletons on Biomechanical Loading of the Lumbar Spine.” Applied Ergonomics 75: 1–7. doi:10.1016/j.apergo.2018.09.006. [PubMed: 30509514]

Poitras I, Dupuis F, Bielmann M, Campeau-Lecours A, Mercier C, Bouyer LJ, and Roy JS. 2019. “Validity and Reliability of Wearable Sensors for Joint Angle Estimation: A Systematic Review.” Sensors 19 (7): 1555. doi:10.3390/s19071555. [PubMed: 30935116]

Raabe ME, and Chaudhari AMW. 2016. “An Investigation of Jogging Biomechanics Using the Full-Body Lumbar Spine Model: Model Development and Validation.” Journal of Biomechanics 49 (7): 1238–1243. doi:10.1016/j.jbiomech.2016.02.046. [PubMed: 26947033]

Robert-Lachaine X, Mecheri H, Larue C, and Plamondon A. 2017. “Validation of Inertial Measurement Units with an Optoelectronic System for Whole-Body Motion Analysis.” Medical & Biological Engineering & Computing 55 (4): 609–619. doi:10.1007/s11517-016-1537-2. [PubMed: 27379397]

Seel T, Raisch J, and Schauer T. 2014. “IMU-Based Joint Angle Measurement for Gait Analysis.” Sensors 14 (4): 6891–6909. doi:10.3390/s140406891. [PubMed: 24743160]

Sen-Gupta Ellora, Wright Donald E., Caccese James W., Wright John A., Jortberg Elise, Bhatkar Viprali, Ceruolo Melissa, Ghaffari Roozbeh, Clason Dennis L., Maynard James P., and Combs Arthur H.. 2019. “A Pivotal Study to Validate the Performance of a Novel Wearable Sensor and System for Biometric Monitoring in Clinical and Remote Environments.” Digital Biomarkers 3 (1): 1–13. doi:10.1159/000493642. [PubMed: 32095764]

Ulrey BL, and Fathallah FA. 2013. “Effect of a Personal Weight Transfer Device on Muscle Activities and Joint Flexions in the Stooped Posture.” Journal of Electromyography and Kinesiology 23 (1): 195–205. doi:10.1016/j.jelekin.2012.08.014. [PubMed: 23021604]

von Glinski Alexander, Yilmaz Emre, Mrotzek Silvia, Marek Eike, Jettkant Birger, Brinkemper Alexis, Fisahn Christian, Schildhauer Thomas A., and Geßmann Jan. 2019. “Effectiveness of an on-Body Lifting Aid (HAL(R) for Care Support) to Reduce Lower Back Muscle Activity during Repetitive Lifting Tasks.” Journal of Clinical Neuroscience 63: 249–255. doi:10.1016/j.jocn.2019.01.038. [PubMed: 30773477]

Waters TR, Putz-Anderson V, Garg A, and Fine LJ. 1993. “Revised NIOSH Equation for the Design and Evaluation of Manual Lifting Tasks.” Ergonomics 36 (7): 749–776. doi:10.1080/00140139308967940. [PubMed: 8339717]

Wesslén J. 2018. “Exoskeleton Exploration: Research, Development, and Applicability of Industrial Exoskeletons in the Automotive Industry.” https://hj.diva-portal.org/smash/record.jsf?pid=diva2%3A1216221&dswid=5543

Weston EB, Alizadeh M, Knapik GG, Wang X, and Marras WS. 2018. “Biomechanical Evaluation of Exoskeleton Use on Loading of the Lumbar Spine.” Applied Ergonomics 68: 101–108. doi:10.1016/j.apergo.2017.11.006. [PubMed: 29409622]

Yin W, Reddy C, Zhou Y, and Zhang X. 2021. “A Novel Application of Flexible Inertial Sensors for Ambulatory Measurement of Gait Kinematics.” IEEE Transactions on Human-Machine Systems 51 (4): 346–354. doi:10.1109/THMS.2021.3086017.

Yin W, Chen Y, Reddy C, Zheng L, Mehta R, and Zhang X. 2022. “Flexible Sensor-Based Biomechanical Evaluation of Passive Low-Back Exoskeleton Use in Lifting.” Proceedings of the Human Factors and Ergonomics Society Annual Meeting 66 (1): 277–279. doi:10.1177/1071181322661203.

Zahabi M, Shahini F, Yin W, and Zhang X. 2022. “Physical and Cognitive Demands Associated with Police in-Vehicle Technology Use: An on-Road Case Study.” Ergonomics 65 (1): 91–104. doi:10.1080/00140139.2021.1960429. [PubMed: 34308789]

Zheng L, Lowe B, Hawke AL, and Wu JZ. 2021. “Evaluation and Test Methods of Industrial Exoskeletons in Vitro, in Vivo, and in Silico: A Critical Review.” Critical Reviews in Biomedical Engineering 49 (4): 1–13. doi:10.1615/CritRevBiomedEng.2022041509.

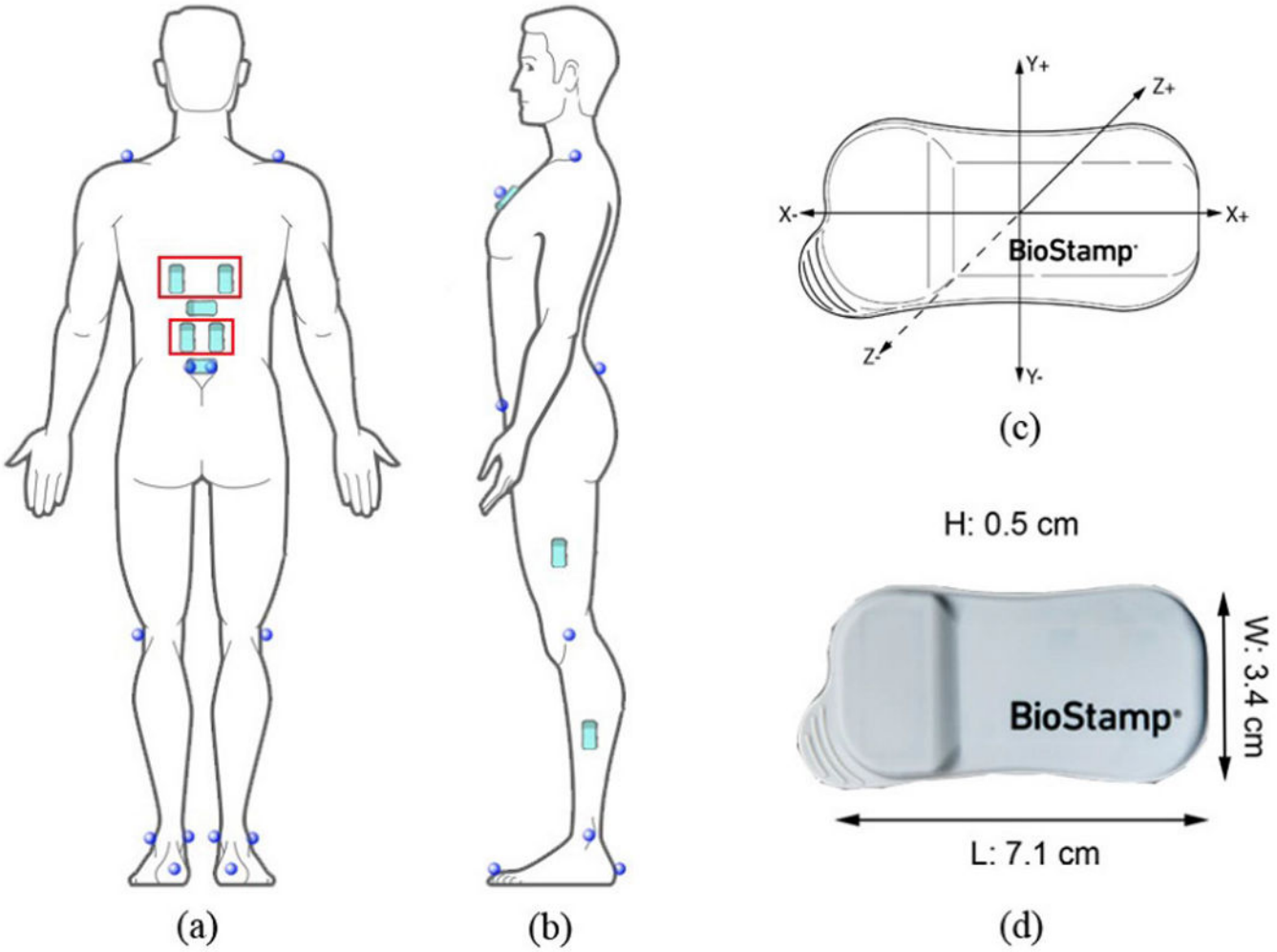

Figure 1.
Sensor and reflective marker placement (a,b) and the sensor's features (c,d). Sensors in red rectangles were used to acquire surface EMG signals while others were used to measure kinematics. Pictures were created by adapting images from MC10 Inc., MA, USA.

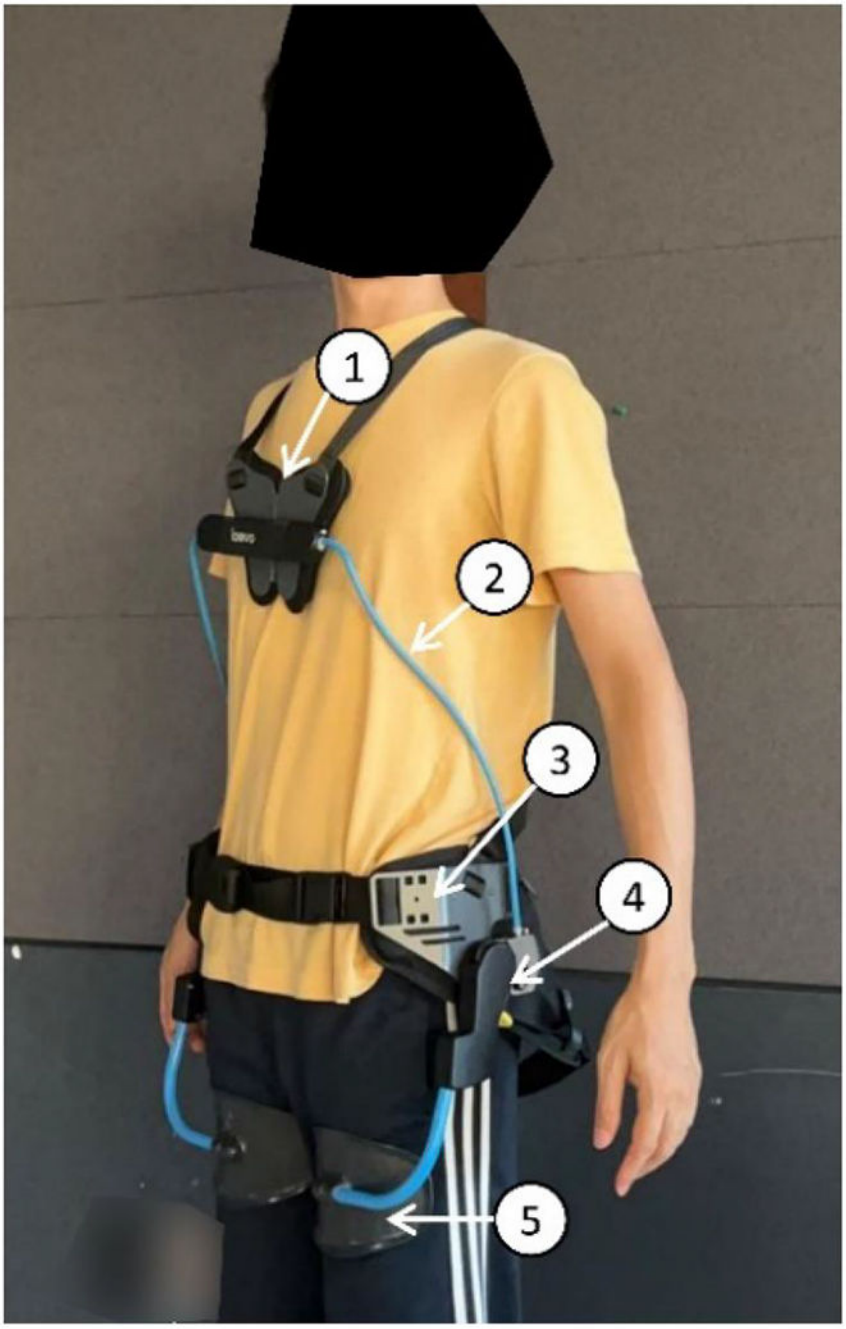

Figure 2.
Laevo V2.5 (Laevo, Delft, The Netherlands). (1) Chest pad, (2) Torso structures, (3) Hip paddings, (4) Spring-loaded joint, and (5) Leg pad.

Figure 3.
A subject performing the squat lifting task with the low-back exoskeleton. BioStamp sensors on the back were directly attached to the skin beneath the exoskeleton.

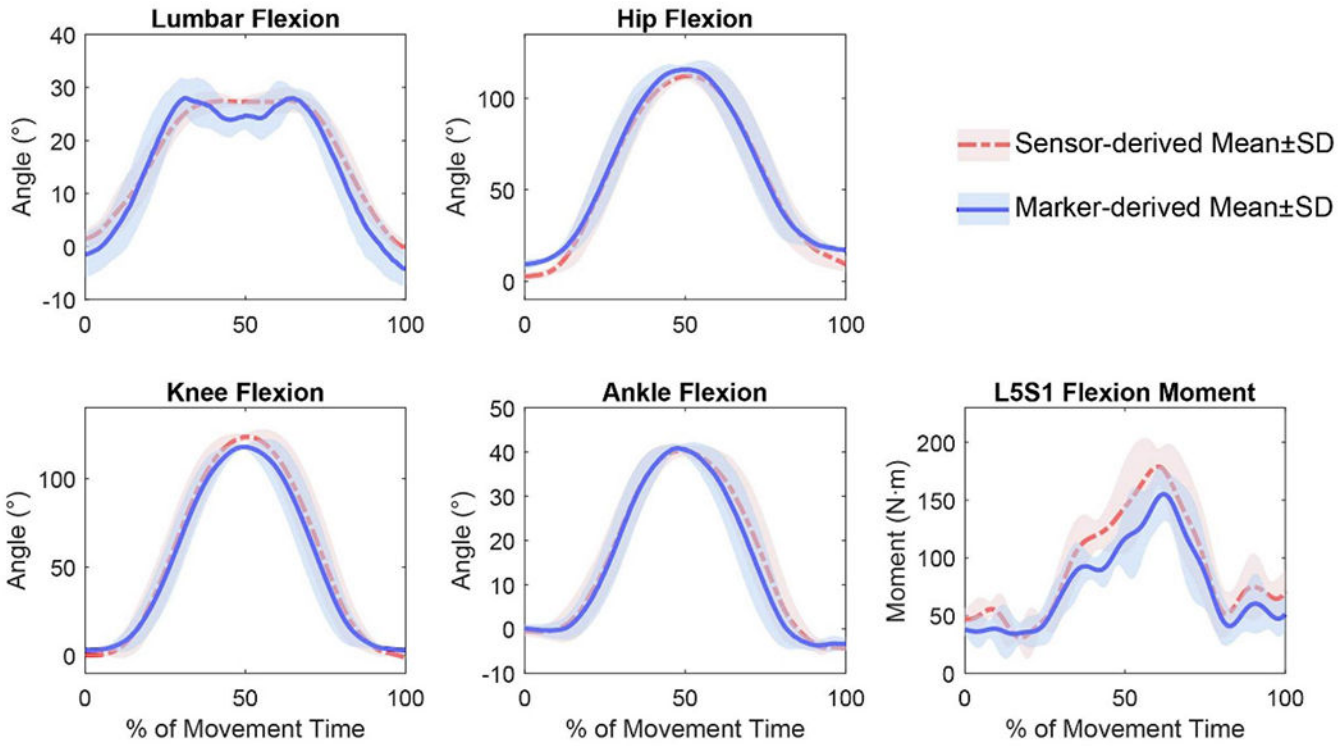

Figure 4.

Joint kinematics and L5S1 moment profiles derived by the conventional marker-based method and proposed sensor-based method for a representative subject (Subject 3). The results of five trials were time-normalised to 0–100% of the lifting task. The mean and standard deviation during each frame were then calculated.

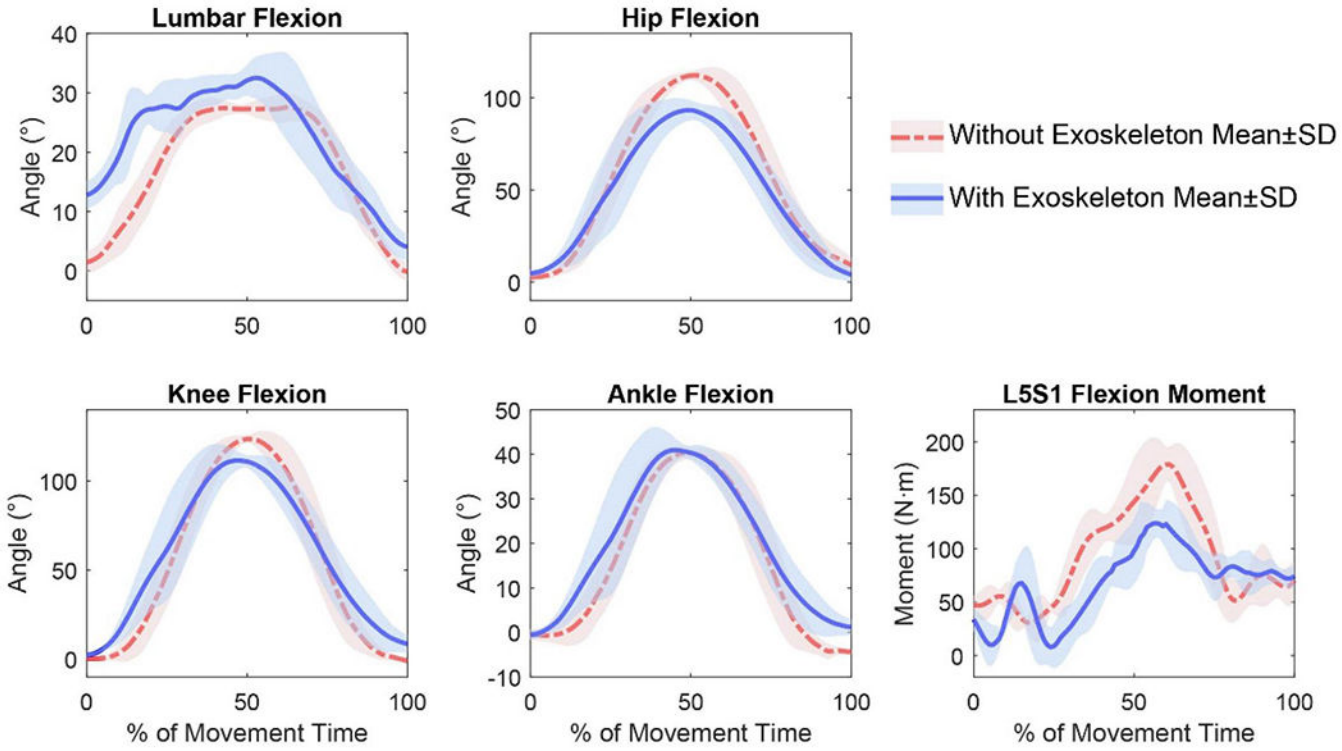

Figure 5.

Joint kinematics and L5S1 flexion moments profiles of a representative subject (Subject 3) comparing conditions WITH and WITHOUT the exoskeleton. All results were derived from flexible sensor measurements. The results of five trials were time-normalised to 0–100% of the lifting task. The mean and standard deviation during each frame were then calculated.

Table 1.

The grand mean and standard deviation (SD) of RMSE and *r* between sensor- and marker-based measurements of each joint flexion angle and L5S1 flexion moment across all lifting trials without the exoskeleton and all subjects.

		Lumbar flexion	Hip flexion	Knee flexion	Ankle flexion	L5S1 flexion moment
RMSE	Mean	7.67°	4.80°	3.99°	3.39°	21.02 N·m
	SD	2.16°	2.11°	1.85°	1.03°	7.63 N·m
r	Mean	0.954	0.995	0.997	0.995	0.926
	SD	0.032	0.005	0.001	0.003	0.047

Table 2.

The mean and standard deviation (SD) of the differences of peak joint angle and L5S1 flexion moment between conditions WITH and WITHOUT the exoskeleton across all subjects.

		Lumbar flexion	Hip flexion	Knee flexion	Ankle flexion	L5S1 flexion moment
Difference (WITH-WITHOUT)	Mean	9.08°	−10.00°	−6.15°	0.44°	−26.97 N·m
	SD	8.32°	9.27°	10.49°	4.82°	18.57 N·m
Statistic t_{11}		3.78	−3.74	−2.03	0.318	−5.03
p-Value		0.003	0.003	0.067	0.757	<0.001

Ergonomics. Author manuscript; available in PMC 2024 October 29.

Table 3.

Mean and standard deviation (SD) of the differences of the peak normalised muscle activities (%baseline) between conditions WITH and WITHOUT the exoskeleton across all subjects.

		LES	TES
Difference (WITH-WITHOUT)	Mean	−15.9	−12.8
	SD	8.6	12.8
Statistic t_{11}		−6.36	−3.47
p-Value		<0.001	0.003